Garrett, D. J., A. L. Saunders, C. McGowan, J. Specks, K. Ganesan, H. Meffin, R. A. Williams and D. A. Nayagam (2015). In vivo biocompatibility of boron doped and nitrogen included conductive-diamond for use in medical implants. Journal of biomedical materials research. Part B, Applied biomaterials. doi:10.1002/jbm.b.33331: [epub ahead of print].

In vivo biocompatibility of boron doped and nitrogen included conductive-diamond for use in medical implants.

David J. Garrett [†,‡], Alexia L. Saunders [†], Ceara McGowan[†], Joscha Specks [§], Kumaravelu Ganesan [‡], Hamish Meffin[ǁ], Richard A. Williams [⊥,#], David A.X. Nayagam [†,⊥,*]

[†] *The Bionics Institute, 384-388 Albert Street, East Melbourne, Victoria 3002, Australia*

[‡] *School of Physics, The University of Melbourne, Victoria 3010, Australia*

[§]*Strategy Engineers GmbH & Co. KG, Prinz-Ludwig-Straße 7, 80333 Munich, Germany*

[ǁ] *NICTA, Department of Electrical and Electronic Engineering, The University of Melbourne, Victoria 3010, Australia*

[⊥] *Department of Pathology, The University of Melbourne, Victoria 3010, Australia*

[#] *Department of Anatomical Pathology, St Vincent's Hospital, Fitzroy, Victoria 3065, Australia*

* *Corresponding Author:* D.A.X. Nayagam, Email: dnayagam@bionicsinstitute.org, Ph: +61 396677500

Abstract

Recently, there has been interest in investigating diamond as a material for use in biomedical implants. Diamond can be rendered electrically conducting by doping with boron or nitrogen. This has led to inclusion of boron doped and nitrogen included diamond elements as electrodes and/or feedthroughs for medical implants. As these conductive device elements are not encapsulated, there is a need to establish their clinical safety for use in implants. This article compares the biocompatibility of electrically conducting boron doped diamond and nitrogen included diamond films and electrically insulating poly crystalline diamond films against a silicone negative control and a boron doped diamond sample treated with stannous octoate as a positive control. Samples were surgically implanted into the back muscle of a guinea pig for a period of 4 - 15 weeks, excised and the implant site sectioned and submitted for histological analysis. All forms of diamond exhibited a similar or lower thickness of

fibrotic tissue encapsulating compared to the silicone negative control samples. All forms of diamond exhibited similar or lower levels of acute, chronic inflammatory, and foreign body, responses compared to the silicone negative control indicating that the materials are well tolerated *in vivo*.

Introduction

Recent advances in the development of medical implants have included various forms of diamond as electrically conducting and passive components. Our particular motivation to conduct this experiment was to establish the clinical safety of the materials which comprise the electrode array of a retinal prosthesis under development by Bionic Vision Australia (BVA).[1, 2] The electrode array is shown in Figure 1, comprising an insulating polycrystalline diamond (PCD) substrate containing 256 nitrogen included ultrananocrystalline diamond (N-UNCD) feedthroughs and electrodes.

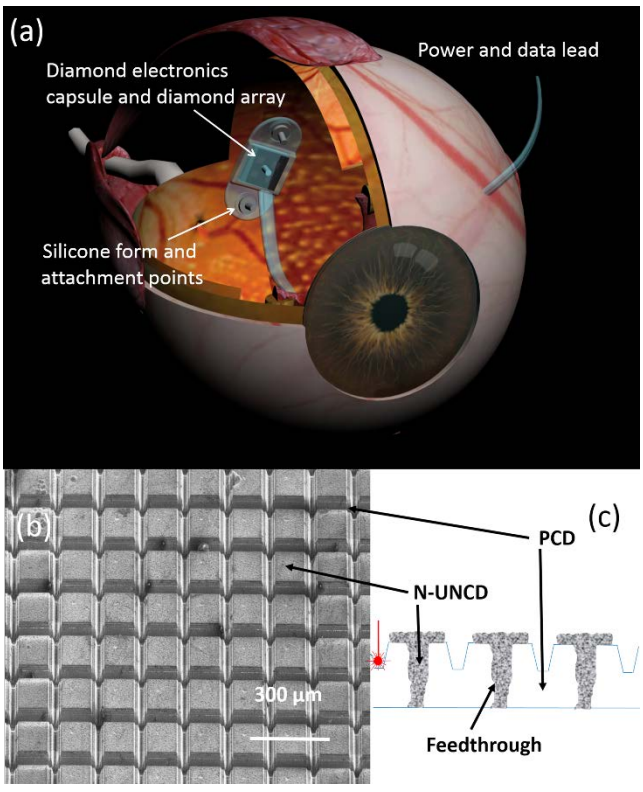

Figure 1. (a) Location and appearance of the BVA retinal prosthesis. (b) SEM image of (b) and internal structure (c) of the PCD / N-UNCD retinal stimulation electrode array.[1, 2]

Boron doped diamond (BDD) has electrochemical properties that position it as a promising electrode material for neural recording.[3] Halpern *et al.* [4] successfully recorded nerve action potentials in a Sea Hare (*Aplysia californica*) using a BBD coated tungsten wire electrode. A

similar electrode system was used by Chan *et al.* [5] to detect the neurotransmitter norepinephrine *in vitro* and to record action potentials directly from the auditory cortex of a Guinea pig. Advances in fabrication methods have led to BDD micro electrode arrays,[6, 7] some targeted specifically towards medical implants.[8] To our knowledge however, no report exists specifically addressing the clinical safety of BDD as an exposed implant material. Boron is not inherently a highly toxic element [9] however boron nitride nanotubes have exhibited cytotoxity *in vitro.*[10] Boron dopant atoms in diamond are bound in the lattice and are not expected to be labile, thus BDD is unlikely to prove cytotoxic. Regardless of these factors it is a requirement that all new medical implant materials be assessed for clinical safety.

Nitrogen included ultrananocrystalline diamond (N-UNCD) is a form of diamond grown by chemical vapour deposition (CVD) in the presence of a percentage of nitrogen gas. The term "ultranano" usually refers to polycrystalline diamond films with diamond crystals of the order of 3-5 nm in size. The films used during this work exhibited conductivities around 2×10^{-4} Ωm and exhibited a distinctive micro and nano-scale structure that we have described previously. [1, 11] Though commonly referred to as nitrogen doped diamond the majority of evidence indicates that the presence of nitrogen in the CVD chamber results in diamond films with more graphitic character and wider grain boundaries accounting for the electrical conductivity of the material. [12, 13] Elemental analysis indicates that very little nitrogen is incorporated in the film,[11] hence the materials is referred to as nitrogen included for the purposes of this article. Unlike BDD, N-UNCD can exhibit relatively high electrochemical capacitance which means it can be safely used as a neural stimulation material.[1, 11] As indicated in Figure 1. Ganesan *et al.* describe a method whereby N-UNCD can be grown within an electrically insulating polycrystalline diamond (PCD) substrate forming hundreds of high density N-UNCD electrodes and hermetic electrical feedthroughs for the specific

application of a retinal prosthesis.[2] *In vitro* assessments of non-conducting forms of UNCD have invariably shown the material to be non-cytotoxic.[14-16] An *in vivo* example of UNCD coated silicon showed that the material was well tolerated in the eye of a Rabbit during six months of implantation.[17] Ariano *et al.* found that GT1-7 neuronal cells on NCD films adhered, proliferated and exhibited healthy Ca^{2+} activity regardless of the surface chemistry (-H or -O atom termination) of the diamond film.[18] In studies where cells were grown on electrically conducting N-UNCD the material is also found to be non-cytotoxic.[19, 20] This evidence, again, suggests that this form of diamond should be well tolerated *in vivo.*

The following is a systematic study directly comparing the clinical safety of BDD and N-UNCD against standard medical grade silicone and electrically insulating PCD. The study is designed to test the passive effect of the materials on surrounding tissue only therefore no electrical connection to the samples was employed. As the major use of electrically conducting diamond in medical implants is likely to be as either recording or stimulating electrodes, the degree of fibrotic encapsulation was targeted as the primary measure of biocompatibility. Histopathological assessment was also conducted to assess the nature of the inflammatory and foreign body response to the implanted materials. Histological response caused by electrical stimulation with diamond electrodes is an important safety concern which will be addressed in future studies

Methods

Materials

PCD mechanical grade was purchased from Element Six Ltd in 8 mm diameter 250 µm thick discs. PCD TM100 (Element Six) thermal grade was purchased as 10 mm x 10 mm × 250 µm plates that were subsequently cut to 8 mm diameter discs using an Oxford Lasers laser cutter.

Heavily doped electrochemistry grade BDD (10^{21} atoms cm^{-3}, 0.5×10^{-3} Ωm) was purchased from Element Six as 8 mm diameter by 250 µm thick discs. N-UNCD samples were prepared by growing a layer of N-UNCD onto a TM100 PCD disc (dimensions above) using previously described methods.[11] Briefly, N-UNCD films approximately 10 - 20 µm thick were grown, in house, by microwave plasma chemical vapour deposition (MPCVD) using a gas mixture of 20% N_2, 79 % Ar and 1 % Methane at a total flow rate of 100 sccm. Chamber pressure was maintained at 80 torr, microwave power was 1 kW and the growth stage was heated to 900 ^{o}C. Silicones used were; SILASTIC biomedical grade silicone sheets (Dow Corning), Bioplexus medical grade silicone sheet (Nusil), Permatex 65AR condensation cure, flowable silicone (Permatex Inc, Connecticut) and MED-1540 condensation cure, flowable silicone (Nusil).

Sample preparation

PCD and BDD samples were cleaned by boiling for at least 5 min in a mixture of either concentrated H_2SO_4: HNO_3: $HClO_4$ 1:1:1 or concentrated H_2SO_4 / $NaNO_3$ salt 10 $mg.mL^{-1}$ to remove graphitic, organic or metallic contamination. N-UNCD samples were not acid boiled as N-UNCD contains a large proportion of graphitic carbon and the acid boiling would lead to significant changes in film structure. All samples were handled with plastic tweezers throughout to avoid metal transfer from tools. Cleaned discs were mounted as shown in Figure 2. Discs were glued to silicone sheet with flowable silicone and a thin bead of flowable silicone was introduced around the edge of the device to cover the edges. Once cured, 10 mm diameter samples were cut with a punch so that the edges of each

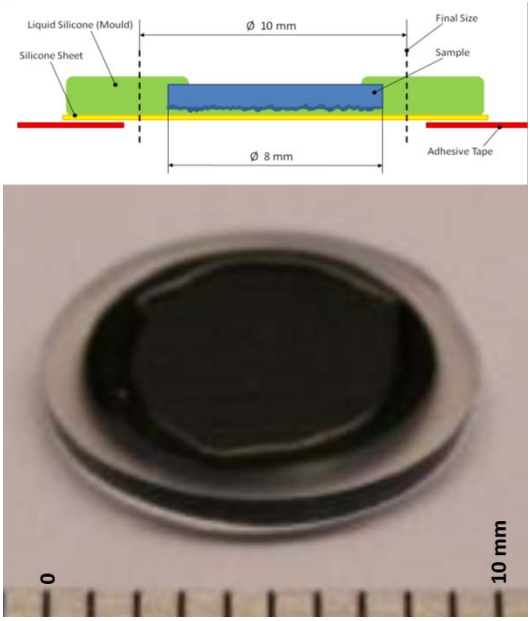

Figure 2. Dimensions and construction of diamond samples

diamond sample were protected by a 1 mm thick halo of silicone. The silicone halo was introduced to reduce the chance of mechanical tissue damage occurring at the sharp edges of the diamond. Negative control samples (silicone) were prepared in the same way as PCD samples except that silicone sheet was attached to both sides of the diamond disc, completely covering it. Thus, the control and diamond samples had the same stiffness. Positive control samples were BDD samples treated by dipping in a solution of the organometallic salt Tin 2-ethylhexanoate; Bis(2-ethylhexanoate) or stannous octoate which is known to cause a strong inflammatory response.[21] A small amount of stannous octoate solution was dropped into the surface of the positive control samples.

Surgical implantation and explantation

The procedures for this study were approved by the Animal Research Ethics Committee of the Royal Victorian Eye and Ear Hospital and complied with both the "Australian Code of Practice for the Care and Use of Animals for Scientific Purposes" and the "Principles of Laboratory Animal Care". Implantation, explantation, tissue preparation and analysis were conducted according the protocol developed by Nayagam *et. al.*[21] Six Guinea pigs were each implanted with six samples according to the locations depicted in Figure 3.

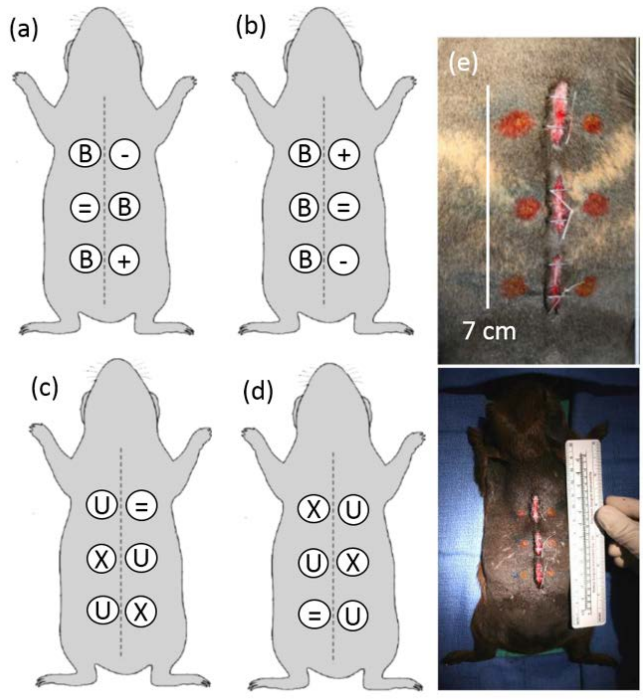

Figure 3. Implant locations for the four guinea pigs included in the study (a-d). (B) = BDD, (U) = N-UNCD, (+) = Stannous Octoate (positive control), (=) = PCD (internal control), (-) = Silicone (negative control). Samples denoted by an (X) were PCD samples that contained the active braze alloy Silver-ABA and are the subject of a separate study that will not be discussed here. Panel (e) shows the location of the three wounds, from two of the subjects, through which the samples were implanted.

The samples were implanted as left / right pairs consisting of one test sample and one control sample. The location of the pairs in relation to the head and tail

of the guinea pig and the left / right orientation of each pair was randomised. The Guinea pigs were anaesthetized with ketamine (Ketamil, Troy Labs, Australia). A single full-thickness ~ 15 mm midline skin incision was made at each implant site. Left and right lateral pockets were opened in the back muscle using blunt dissection along cleavage planes and the implants were inserted. The Guinea pigs were recovered, returned to their housing and allowed to move freely for a period of either 4 (BDD, Stannous Octate, PCD) or 15 weeks (N-UNCD). N-UNCD was implanted for a longer period as the material was earmarked for use as the stimulating materials in a visual prosthesis.[1, 2, 11] After the implant period the animals were euthanized by an overdose of ketamine and xylazine (Ketamil, Xylazil, Troy Labs, Australia) and transcardially perfused with 37 °C Heparinised Saline followed by 4 °C neutral buffered formalin (NBF). Gross dissection involved removal of a block of muscular tissue surrounding each implant. The tissue was marked with red, green and blue Davidson's permanent tissue marking dye (Bradley Products Inc, Bloomington) to identify the orientation of the sample during subsequent processing. The tissue was post fixed in 10% NBF and stored at 4°C. PCD samples containing Silver-ABA braze (Westgo metals) were also present for Guinea pigs implanted with N-UNCD. This was part of a separate study and will not be discussed here.

Histological preparation and analysis

Preparation, sectioning, analysis and measurements were conducted following the protocol developed by Nayagam et al. [21]After 4 days post fixation in formalin at 4 ^{o}C, the tissue blocks were removed and trimmed to reveal the edges of the various

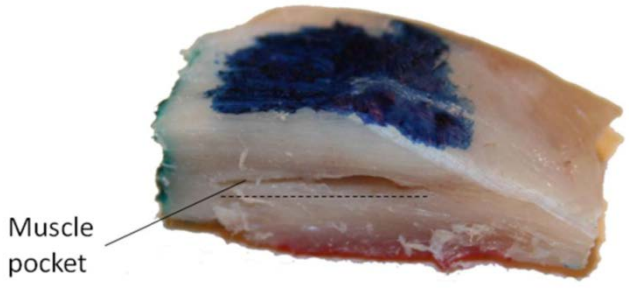

Figure 4. An example of a partially fixed tissue block after implantation, removal of the implant and dye orientation markings. The dotted line represents the extent of the implant pocket (dotted line is located slightly ventral to the pocket).

samples. An incision was made parallel to the sample orientation and the samples removed. The samples were removed because the diamond is too hard to be sectioned in situ. Figure 4 shows an example of a tissue block following removal of the sample.

Following a further three days in formalin at 4 ^{o}C the tissue blocks were embedded in Histowax paraffin using an automatic tissue processor (Leica Microsystems GmbH, Wetzlar). Twelve 4 µm thick paraffin embedded tissue sections were collected approximately through the centre of the implant pocket. For samples containing diamond a mathematical method (equation 1.) based on the width of the tissue pocket was used to determine the length of tissue in contact with diamond.

$$L_d = Cos\left(Sin^{-1}\left(\frac{Sin\left(Cos^{-1}\left(\frac{L_s}{2\,R_s} \right) R_s \right)}{R_d} \right) \right) R_d \qquad \text{Equation 1.}$$

Where L_d = Length of tissue against diamond, L_s = the total width of the tissue pocket after sectioning, R_s = radius of sample including silicone overmould and R_d = radius of exposed diamond.

Four high quality sections were selected per block using a standardised naïve scoring protocol. The samples were stained with either Hematoxylin & Eosin (H & E) stain or Masson's Trichrome Stain. The sections were imaged, analysed and evaluated using AxioVision LE software (Carl Zeiss Ag). Between four and ten (depending on the quality of the sections) fibrotic encapsulation thickness measurements per sample side were collected. Samples that appeared substantially tilted in the pocket after sectioning were not included as the tilt adds an intractable error to the encapsulation measurement. Following encapsulation measurements, the sections were scored in a blind fashion by an independent pathologist. The extent of acute inflammation, chronic inflammation and foreign body / histocytic

response for each sample was evaluated and scored on a scale from 0 (no reponse) to 4 (severe response).

Statistical analysis

Encapsulation measurements are reported as range, upper and lower quartile and median because the populations are not expected to follow a normal distributions. Two tailed, Mann-Whitney and standard unpaired student-t tests between the collated populations of encapsulation thickness measurements across all samples were conducted to compare N-UNCD, BDD, PCD and Silicone encapsulation.

Results

Encapsulation measurement

The thickness of the fibrous encapsulation surrounding each of the implants was measured. Figure 5 shows typical images of Trichrome stained slices from which the measurements were taken. The tissue depicted previously containined (a) BDD, (b) N-UNCD, (c) Silicone (negative control), (d) PCD (internal control) and (e) stannous octoate treated BDD (positive control) samples. The blue colour in the images indicates fibrous tissue encapsulation. The images show a thin line of fibrous encapsulation (blue) for all samples with exception of

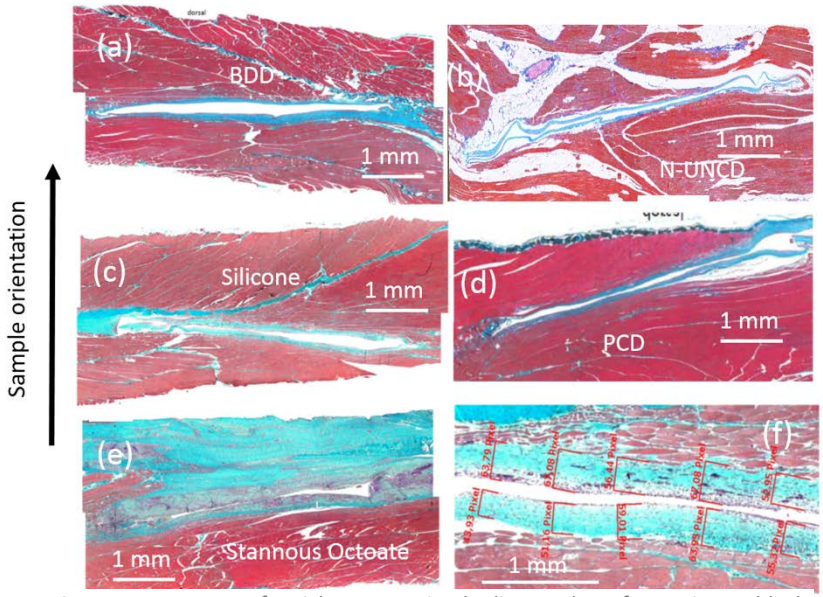

Figure 5. Images of Trichrome stained slices taken from tissue blocks previously containing (a) BDD, (b) N-UNCD, (c) Silicone, (d) PCD and (e) Stannous Octoate. (f) Shows a high magnification image of a silicone (negative control sample) marked with the pixel count measurements used to evaluate fibrous encapsulation thickness.

stannous octoate treated samples where scarring and fibrous encapsulation was more extensive.

Figure 6 is a bar and whisker graph indicating the median, upper and lower quartile and range of the collated encapsulation values measured for each of the sample types. The number of measurement recorded for each of the different sample types was; N-UNCD = 23 (5 of 6 measured), BDD = 45 (5 of 6 measured), Silicone = 50 (5 measured, double sided) , PCD = 15 (2 measured), Stannous Octoate (2 estimated). The median encapsulation thickness increased in the sample order; N-UNCD < BDD < PCD < Silicone<stannous octoate. Five of the six N-UNCD samples implanted were sufficiently level to be measured yielding a median encapsulation thickness of 16 µm. Of the six BDD samples five were measured yielding a median encapsulation of 86 µm. BDD samples adjacent to stannous octoate exhibited increased fibrous encapsulation. The collated PCD, silicone and stannous octoate results yielded median encapsulation thickness values of 134, 149 and >1400 µm respectively. Both the Man-Whitney (1 % significance) and Student-T test ($P < 0.001$) returned the results that fibrotic encapsulation over N-UNCD was significantly less than BDD. The same tests also indicated that encapsulation around BDD was significantly less than silicone. Mann Whitley and Student-t ($p=0.011$) tests both indicated that encapsulation

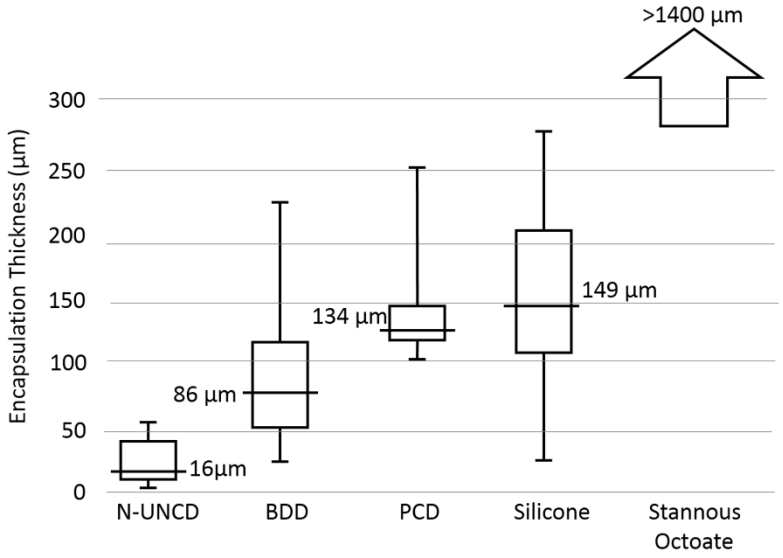

Figure 6. Bar and whisker graph indicating the range, upper and lower quartiles and median thickness of fibrotic encapsulation recorded across all samples.

over BDD was significantly less than PCD at 5% significance level though with the lower number of PCD measurements, this result is less conclusive. The degree of encapsulation surrounding stannous octoate samples was too severe for accurate measurements therefore values are an estimate only.

Pathologist's findings

Figure 7 shows examples of slices previously containing stannous octoate samples (a),(b) and N-UNCD samples (c),(d) after H & E staining (a,c) and Trichrome staining (b,d). The bar graph shows the collated pathologist scores for all sample types for the categories; acute and chronic inflammation and foreign body / histocytic response. Stannous octoate samples are shown to best illustrate the various types of reponse identified by the pathologist and N-UNCD to illustrate a very low response. In Figure 7 (a) (H & E stain), the nuclei of viable cells stain a dark blue/purple and have surrounding eosinophilic or amphophilic cytoplasm. The necrotic material contains fragmented nuclear and cytoplasmic debris together with necrotic connective tissue fragments and appears as structure-less areas with amorphous pink masses admixed with the fragmented nuclear material. In Trichrome

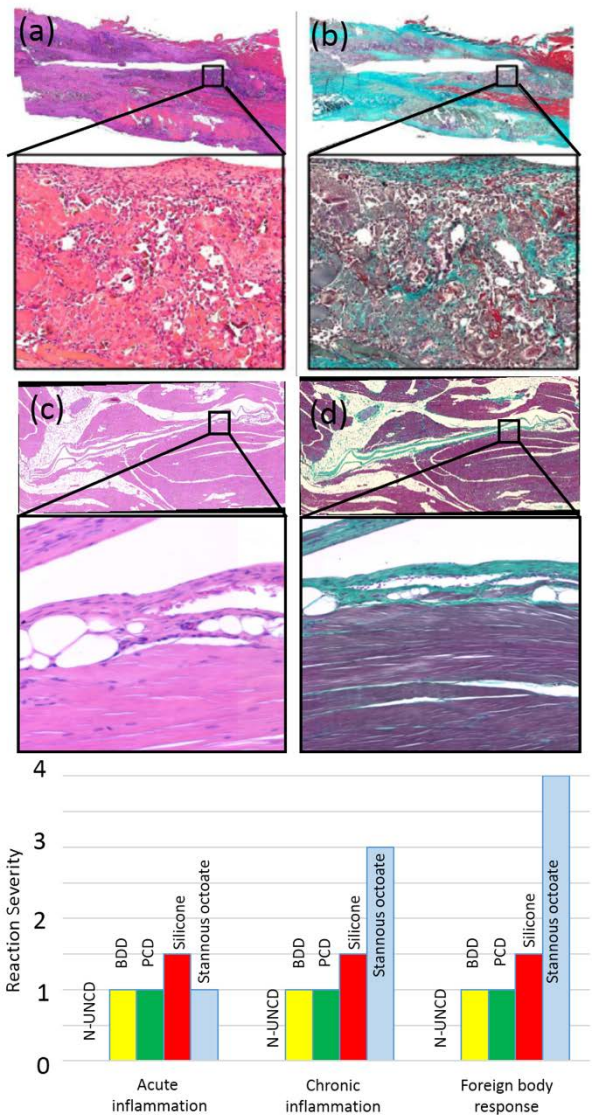

Figure 7. Examples of low and high magnification images of tissue slices stained with either H & E (a), (c) or Trichrome stain (b),(d). (a) and (b) show tissue previously adjacent to a stannous octoate positive control and (c) and (d) show tissue previously adjacent to an N-UNCD sample. The bar graph shows the pathologist scores for tissue adjacent to all sample types, including medical grade silicone, in the categories: acute and chronic inflammatory response; and foreign body reaction. A score of 0 indicates no response and a score of 4 indicates a severe response.

stained samples (example shown in Figure 7 (b)) the necrotic material appears heterogeneous and smudged grey, collagenous connective tissue stains blue and skeletal muscle red. Where inflammation was extensive the pathologist identified inflammatory cells, neutrophils and lymphocytes and phagocytic and foreign body reaction cells including macrophages and foreign body giant cells. Neutrophils indicate acute inflammatory response and were found in low numbers in all samples. Cells consistent with chronic ongoing inflammation, lymphocytes and monocytes, were found in low numbers on BDD, N-UNCD, PCD and silicone samples and in high numbers in stannous octoate treated samples. Foreign body response was evaluated by the presence and appearance of macrophages and the degree to which macrophages coalesce into giant cells. A small foreign body response, immediately adjacent to all implants except N-UNCD was observed but was much more extensive in those treated with stannous octoate.

Discussion

Passive histological reactions to implanted materials are generally common to any anatomical placement – for example Stannous Octoate is poorly tolerated in any location. The present study is a first order evaluation of material biocompatibility where we have attempted to decouple the material histological response from any response caused by electrical or mechanical factors. Hence we protected the sharp edges of the device with silicone and chose a resilient and stable location for implantation. Clearly the eye is a much more delicate environment than muscle tissue and any device would need to be carefully designed to minimize mechanical damage to the retina for example. The protocol developed here is a straight forward method to assess the safety of new materials to guide device designers decision making concerning including them in a future device.

Fibrotic encapsulation was used as the primary method of assessing device utility because of the likelihood that conducting forms of diamond will be used as either neural recording or stimulating electrodes. When a neuron fires an action potential it perturbs the environment around itself and generates an electric field. This field can produce a detectable voltage change in a nearby recording electrode. The strength of the electric field generated by the neuron attenuates rapidly with distance thus high quality recordings are only possible if electrodes are close to the target neurons. Fibrotic encapsulation of recording electrodes increases the distance between the electrode and decreases ion permeability dramatically decreasing recording quality,[22, 23] therefore minimal fibrotic response is desirable. Fibrotic encapsulation around stimulating electrodes also increases distance and decrease permeability from electrode to cell and raises the amount of charge that is required to electrically stimulate neurons. Use of low charge in neural stimulation implants is desirable for safety (high charge can damage tissue), power consumption and voltage compliance reasons among others. N-UNCD samples exhibited significantly less median fibrotic encapsulation than any of the other samples measured. In hind sight the stannous octoate positive controls used in this study were too strong and clearly increased the degree of encapsulation over the two adjacent BDD samples. Despite the impact of the stannous octoate, BDD still exhibited significantly less encapsulation than silicone though the difference was not so marked as that between N-UNCD and silicone.

Kromka *et al.* measure the surface potential of BDD with varying levels of boron dopant and found that high dopant level samples had more positive surface potentials and observed enhanced adhesion, growth and maturation of MG osteoblast cells on highly doped samples.[24] Grausova *et al.* also observe enhanced growth and differentiation of MG 63 cells on nanodiamond films and a further growth enhancement when the films were heavily boron doped.[25] Bacokava *et al.* in their recent review attribute enhanced cell adhesion and growth

on positively charged surface to presence of negatively charged cell adhesion molecules which are attracted to positively charged surfaces.[26] These observations and conclusions are drawn from highly controlled *in vitro* experiments and may not be applicable to our observations *in vivo*. It is evident however that surface charge can affect the biochemistry of cells in contact and therefore may in turn affect the inflammatory response of an implant. N-UNCD films were electrically conducting and also have a high degree of nano-scale and micro-scale roughness that occurs during the growth process. Surface roughness can also greatly affect bacterial adhesion and biofilm formation on medical implants [27] therefore we cannot attribute reduced inflammatory response to conductivity alone for this material. The extended implant time for this material (15 weeks) could have affected the result though fibrotic encapsulation over an implant in a muscle is unlikely to reduce with time. The minimal inflammatory response exhibited by all the forms of diamond tested, is entirely consistent with previous *in vitro* cytotoxicity studies and consistent with the lack of toxicity of the chemicals composing the films. The study stands as strong evidence that conducting diamond in all the forms tested is likely to exhibit less fibrotic encapsulation and histo/pathological response *in vivo* than medical grade silicone and is therefore an appropriate material for implantation.

Conclusion

After 4-15 weeks implantation in the back muscle of a Guinea pig BDD and N-UNCD samples induced less fibrotic encapsulation than medical grade silicone. An independent pathologist report scored BDD and N-UNCD implant sites as containing less or a similar degree of acute and chronic inflammation and foreign body response than medical grade silicone controls. These results indicate that both BDD and N-UNCD are safe materials for implantation. All conducting diamond samples exhibited less fibrotic encapsulation than silicone which suggests enhanced biocompatibility of conducting diamond.

Acknowledgements

DJG is supported by ARC DECRA grant DE130100922.The Bionics Institute acknowledges the support they receive from the Victorian Government through its Operational Infrastructure Program. NICTA is funded by the Australian Government as represented by the Department of Broadband, Communications and the Digital Economy and the Australian Research Council through the ICT Centre of Excellence program. This research was supported by the Australian Research Council (ARC) through its Special Research Initiative (SRI) in Bionic Vision Science and Technology grant to Bionic Vision Australia (BVA).

References

1. Hadjinicolaou AE, Leung RT, Garrett DJ, Ganesan K, Fox K, Nayagam DAX, Shivdasani MN, Meffin H, Ibbotson MR, Prawer S, O'Brien BJ. Electrical stimulation of retinal ganglion cells with diamond and the development of an all diamond retinal prosthesis. Biomaterials. 2012; 33: 5812-5820
2. Ganesan K, Garrett DJ, Ahnood A, Shivdasani MN, Tong W, Turnley AM, Fox K, Meffin H, Prawer S. An all-diamond, hermetic electrical feedthrough array for a retinal prosthesis. Biomaterials. 2014; 35: 908-915
3. Zanin H, May PW, Fermin DJ, Plana D, Vieira SMC, Milne WI, Corat EJ. Porous Boron-Doped Diamond/Carbon Nanotube Electrodes. Acs Applied Materials & Interfaces. 2014; 6: 990-995
4. Halpern JM, Cullins MJ, Chiel HJ, Martin HB. Chronic in vivo nerve electrical recordings of Aplysia californica using a boron-doped polycrystalline diamond electrode. Diam. Relat. Mat. 2010; 19: 178-181
5. Chan HY, Aslam DM, Wiler JA, Casey B. A Novel Diamond Microprobe for Neuro-Chemical and -Electrical Recording in Neural Prosthesis. J. Microelectromech. Syst. 2009; 18: 511-521
6. Cottance M, Nazeer S, Rousseau L, Lissorgues G, Bongrain A, Kiran R, Scorsone E, Bergonzo P, Bendali A, Picaud S, Joucla S, Yvert B, Ieee, *Diamond Micro-Electrode Arrays (MEAs): a new route for in-vitro applications*. 2013 Symposium on Design, Test, Integration and Packaging of Mems/Moems (Ieee, New York, 2013).
7. Bonnauron A, Saada S, Rousseau L, Lissorgues G, Mer C, Bergonzo P. High aspect ratio diamond microelectrode array for neuronal activity measurements. Diam. Relat. Mat. 2008; 17: 1399-1404
8. Bergonzo P, Bongrain A, Scorsone E, Bendali A, Rousseau L, Lissorgues G, Mailley P, Li Y, Kauffmann T, Goy F, Yvert B, Sahel JA, Picaud S. 3D shaped mechanically flexible diamond microelectrode arrays for eye implant applications: The MEDINAS project. Irbm. 2011; 32: 91-94
9. Hasegawa R, Hirata-Koizumi M, Dourson ML, Parker A, Ono A, Hirose A. Safety assessment of boron by application of new uncertainty factors and their subdivision. Regul. Toxicol. Pharmacol. 2013; 65: 108-114

10. Horvath L, Magrez A, Golberg D, Zhi CY, Bando Y, Smajda R, Horvath E, Forro L, Schwaller B. In Vitro Investigation of the Cellular Toxicity of Boron Nitride Nanotubes. ACS Nano. 2011; 5: 3800-3810
11. Garrett DJ, Ganesan K, Stacey A, Fox K, Meffin H, Prawer S. Ultra-nanocrystalline diamond electrodes: optimization towards neural stimulation applications. J. Neural Eng. 2012; 9:
12. Birrell J, Carlisle JA, Auciello O, Gruen DM, Gibson JM. Morphology and electronic structure in nitrogen-doped ultrananocrystalline diamond. Appl. Phys. Lett. 2002; 81: 2235-2237
13. Birrell J, Gerbi JE, Auciello O, Gibson JM, Gruen DM, Carlisle JA. Bonding structure in nitrogen doped ultrananocrystalline diamond. J. Appl. Phys. 2003; 93: 5606-5612
14. Amaral M, Dias AG, Gomes PS, Lopes MA, Silva RF, Santos JD, Fernandes MH. Nanocrystalline diamond: In vitro biocompatibility assessment by MG63 and human bone marrow cells cultures. J. Biomed. Mater. Res. Part A. 2008; 87A: 91-99
15. Amaral M, Gomes PS, Lopes MA, Santos JD, Silva RF, Fernandes MH. Nanocrystalline diamond as a coating for joint implants: Cytotoxicity and biocompatibility assessment. J. Nanomater. 2008; 9
16. Bajaj P, Akin D, Gupta A, Sherman D, Shi B, Auciello O, Bashir R. Ultrananocrystalline diamond film as an optimal cell interface for biomedical applications. Biomed. Microdevices. 2007; 9: 787-794
17. Xiao XC, Wang J, Liu C, Carlisle JA, Mech B, Greenberg R, Guven D, Freda R, Humayun MS, Weiland J, Auciello O. In vitro and in vivo evaluation of ultrananocrystalline diamond for coating of implantable retinal microchips. J. Biomed. Mater. Res. Part B. 2006; 77B: 273-281
18. Ariano P, Budnyk O, Dalmazzo S, Lovisolo D, Manfredotti C, Rivolo P, Vittone E. On diamond surface properties and interactions with neurons. Eur. Phys. J. E. 2009; 30: 149-156
19. Thalhammer A, Edgington RJ, Cingolani LA, Schoepfer R, Jackman RB. The use of nanodiamond monolayer coatings to promote the formation of functional neuronal networks. Biomaterials. 2010; 31: 2097-2104
20. Specht CG, Williams OA, Jackman RB, Schoepfer R. Ordered growth of neurons on diamond (vol 25, pg 4073, 2004). Biomaterials. 2005; 26: 828-828
21. Nayagam DAX, Williams RA, Chen J, Magee KA, Irwin J, Tan J, Innis P, Leung RT, Finch S, Williams CE, Clark GM, Wallace GG. Biocompatibility of Immobilized Aligned Carbon Nanotubes. Small. 2011; 7: 1035-1042
22. Saxena T, Karumbaiah L, Gaupp EA, Patkar R, Patil K, Betancur M, Stanley GB, Bellamkonda RV. The impact of chronic blood-brain barrier breach on intracortical electrode function. Biomaterials. 2013; 34: 4703-4713
23. Karumbaiah L, Saxena T, Carlson D, Patil K, Patkar R, Gaupp EA, Betancur M, Stanley GB, Carin L, Bellamkonda RV. Relationship between intracortical electrode design and chronic recording function. Biomaterials. 2013; 34: 8061-8074
24. Kromka A, Grausova L, Bacakova L, Vacik J, Rezek B, Vanecek M, Williams OA, Haenen K. Semiconducting to metallic-like boron doping of nanocrystalline diamond films and its effect on osteoblastic cells. Diam. Relat. Mat. 2010; 19: 190-195
25. Grausova L, Kromka A, Burdikova Z, Eckhardt A, Rezek B, Vacik J, Haenen K, Lisa V, Bacakova L. Enhanced Growth and Osteogenic Differentiation of Human Osteoblast-Like Cells on Boron-Doped Nanocrystalline Diamond Thin Films. PLoS One. 2011; 6: 17
26. Bacakova L, Filova E, Parizek M, Ruml T, Svorcik V. Modulation of cell adhesion, proliferation and differentiation on materials designed for body implants. Biotechnol. Adv. 2011; 29: 739-767
27. Desrousseaux C, Sautou V, Descamps S, Traore O. Modification of the surfaces of medical devices to prevent microbial adhesion and biofilm formation. J. Hosp. Infect. 2013; 85: 87-93